ELSEVIER

Journal of Nuclear Materials 289 (2001) 80–85

journal of nuclear materials

www.elsevier.nl/locate/jnucmat

Structural stability of irradiated ceramics

Paolo M. Ossi *

INFM – Dipartimento di Ingegneria Nucleare, Politecnico di Milano, Via Ponzio 34/3, 20133 Milano, Italy

Abstract

Using the segregation-charge transfer (SCT) atomistic model, nucleation of crystalline or amorphous phases is modelled in irradiated binary oxide films, where the bombardment conditions are suitable to the formation of dense collision cascades. Non-equilibrium compositional and electronic density profiles develop at the interface between a cascade and the surrounding crystalline matrix, as a consequence of interface enrichment of one of the film constituents. Electronic density relaxation to metastable equilibrium is treated schematically by local charge transfer reactions (CTR), each involving a pair of dissimilar atoms of the initial compound that constitute a dimer of an effective compound. The energy cost to produce an effective compound dimer, the difference of formation enthalpy between effective and initial compounds, and the local strain associated with a CTR are calculated for a set of 22 oxides, out of which 11 are vitrified and 11 remain crystalline under ion bombardment. Qualitative differences are found in the parameter trends between the two groups of compounds.

PACS: 61.80.Az; 61.80.Jh; 61.82.Ms

1. Introduction

At the beginning of the 20th century, some initially crystalline silicates were observed to lose their structural order when subjected to energetic particle irradiation [1]. Much experimental work has since accumulated, and it is now accepted that easily amorphizable non-metallic compounds include both covalently bonded solids with simple crystalline structure and more complex ionic compounds; in either case, charge localization and steric hindrances on bonding are considered to be responsible for the crystal disruption. Bombardment-induced vitrification is the consequence of the competition between accumulation of radiation damage up to increasingly higher levels and ability of the solid to relax disorder, thus restoring the crystalline structure. However, the experimentally observed differences in amorphization susceptibility among structurally similar non-metallic compounds remain unexplained by the above picture and led to empirical criteria to interpret whether a specific material would amorphize under irradiation. In particular, in covalently bonded irradiated solids, bond ionicity and melting temperature were used as parameters to rationalize amorphization [2].

Such criteria do not take into account those mechanisms, such as chemical disordering and defect formation, migration and accumulation, that give rise to a free energy increase ΔG_{irr} of the bombarded target, up to a point where it surpasses the free energy difference $\Delta G_{\mathrm{c}\rightarrow\mathrm{a}}$ between the equilibrium crystalline state and the amorphous state. The importance of chemical disordering in driving amorphization was assessed in detail in electron-irradiated ceramics [3]. Chemical disordering, besides going with the crystal to amorphous (c → a) transformation, in metallic systems even precedes vitrification. This is confirmed by the combination of structural observations (X-ray diffraction and transmission electron microscopy) and Brillouin scattering measurements on ion-bombarded metallic alloys [4].

The second important mechanism of crystal destabilization is provided by excess point defect accumulation. When vacancies and interstitials are produced in separated regions during irradiation, e.g. when heavy ion bombardment results in cascade formation, this mechanism is favoured. Also, the amorphization process is preferentially initiated at lattice imperfections, such as grain boundaries, dislocations and free surfaces [5].

* Tel.:+390-2 23996319; fax:+390-2 23996309.
E-mail address: paolo.ossi@polimi.it (P.M. Ossi).

0022-3115/01/$ - see front matter
PII: S0022-3115(00)00685-1

The atomistic segregation-charge transfer (SCT) model, which has been successfully applied to interpret the structural stability of a great number of irradiated, implanted, or ion-mixed metallic alloys [6], as well as to nitrides and carbides [7], is here extended to analyse the structural stability of 22 irradiated binary oxides whose behaviour under ion bombardment is known. A presentation of the main features of the model, which tries to take into account the relevant processes arising during the interaction between an incoming energetic massive projectile and the atoms of the bombarded binary compound A_xB_y, is also provided.

2. Theory

Given a binary A_xB_y compound, called the initial (i) compound, it is assumed in the SCT model that upon bombardment well-developed, but still non-overlapping displacement cascades are produced in it along the ion track. For about 10^{-13} s after ion impact, a cascade is a region of concentrated displacement damage. Towards the end of this ballistic regime, when the energy of higher order recoils lies between the displacement energies $E_d(A)$ and $E_d(B)$ (e.g., $E_d(A) < E_d(B)$), only atoms of the constituent with lower E_d value (in the example, A atoms) can be displaced. As a result, at the end of the ballistic regime, the fraction of displaced A atoms with respect to all displaced atoms, is greater than the initial A constituent atomic fraction, i.e. x. Further target evolution involves progressive energy degradation down to the thermal spike regime (10^{-11} s), which is characterized by short-range random atomic motions and freezing of mutually competing local liquid-like configurations at a rate of order 10^{14} K s^{-1}. During this stage, ideal conditions are met to easily nucleate metastable, even amorphous phases. Each cascade, including a few thousand atoms, is embedded in the crystalline solid matrix, adiabatically unperturbed during the lifetime of the cascade. We pay attention to the evolution of a single cascade as sketched in Fig. 1, with the hypothesis that it is formed in a compositionally homogeneous target volume, so that the initial cascade stoichiometry coincides with the average compound stoichiometry. Such a condition is reasonable given the statistical nature of the damage produced by the high number of incident ions.

Before describing the cascade history, we recall that, in general, the high temperature surface composition of a binary compound kept in thermal equilibrium differs from the bulk one due to equilibrium segregation. Even more, when both data for radiation-induced segregation and for equilibrium segregation are available for a given compound, the segregating constituent coincides in both conditions and is the constituent with the lower surface energy γ [8]. On this basis, SCT model assumes that the matrix–cascade interface is equivalent to a free surface and that ion bombardment causes Gibbsian segregation of the constituent with lower γ at such an interface. Indeed, this is a true discontinuity region: at a free surface a discontinuity occurs between the crystal and vacuum; at the interface in question, the two phases are the crystal and the liquified cascade volumes [9].

The choice of the segregating constituent is dictated by experimental data [10] and goes in the sense of system stabilization. Indeed, interface segregation causes a chemically different surface to form, as shown in Fig. 1(b); when the constituent with lower surface energy is involved, the highest possible energy is absorbed from the cascade region. Although in ionic and covalently bonded compounds the displacement energy shows a dependence on chemical bonding, γ values in general scale with E_d values along the periodic table [11]. A coherent explanation for the interface enrichment is

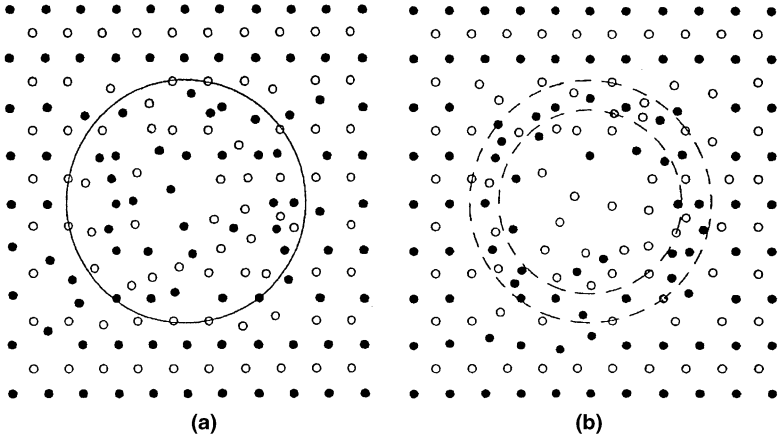

Fig. 1. (a) Schematic cross-section of a collision cascade. The line encloses the most severely disordered region. (b) Preferential segregation at cascade–matrix interface, as represented by the dashed ring. (•) Segregating constituent.

supplied by both the above pictures. In the example, $E_d(A)$ is lower than $E_d(B)$ and γ_A is lower than γ_B; thus the spike–matrix interface is enriched in the A constituent. Segregation evolves as

$$\frac{c_s^{\infty}(B)}{c_s^{\infty}(A)} = \frac{c_b^{\infty}(B)}{c_b^{\infty}(A)} \exp(\Delta G^{seg}/k_B T), \tag{1}$$

where the c_s^{∞} 's are the equilibrium surface concentrations of A and B, the c_b^{∞} 's the bulk concentrations in the initial compound, ΔG^{seg} the segregation contribution to the free energy, and k_B is the Boltzmann constant.

Thus, localized segregation events yield system energy lowering, formation of a composition gradient (the cascade–matrix interface is enriched in the segregating constituent and in turn the cascade core is depleted in the same constituent), and a non-equilibrium electronic density profile, as a consequence of the composition gradient.

The partial re-equilibration of the electronic density profile is simulated by elementary charge transfer reactions (CTRs) between dimers of atoms of A_xB_y. The CTR scheme simulates the presumably very complicated mechanisms of charge re-equilibration, which persist over the timescale of spike evolution, viz. 10^{-12}–10^{-11} s. Supposing that: (1) γ_A is lower than γ_B, (2) in each CTR *one* neutral A atom (atomic number Z_A) and *one* neutral B atom (atomic number Z_B) are involved, and (3) one electron is transferred from atom B of the non-segregating constituent to atom A of the segregating species, we obtain the CTR

$$AB \overset{\gamma_A > \gamma_B}{\rightarrow} \begin{matrix} A + 1e^- \rightarrow A^- \\ B - 1e^- \rightarrow B^+. \end{matrix} \tag{2a}$$

Conversely, if γ_A is higher than γ_B

$$AB \overset{\gamma_A > \gamma_B}{\rightarrow} \begin{matrix} A - 1e^- \rightarrow A^+ \\ B + 1e^- \rightarrow B^-. \end{matrix} \tag{2b}$$

Such a rather crude atomistic approach is justified by the high energy of the spike. A^-, B^+, A^+, B^- are singly charged ions. They are called effective elements and are introduced into the matrix in pairs, as dimers, being considered to be the smallest possible unit of the equiatomic $[(Z_A+1)(Z_B-1)], \text{or} [(Z_A-1)(Z_B+1)]$ compound, called the effective (e) compound. Note that both CTRs go in the direction of shell closing in both atoms. Indeed γ values are increasingly lower in elements with progressively filled electronic shells. We observe that a CTR occurs also between elements with the same degree of outer shell filling due to their different electronegativities [12].

It is possible to evaluate the energy cost ΔE_{e^-} (i → e) needed to obtain an effective compound dimer. For this purpose we use the electron energies of the pure elements [13]. For example, for the CTR in Eq. (2a)

$$\Delta E_{e^-} = \Delta E(A \rightarrow A^-) + \Delta E(B \rightarrow B^+), \tag{3a}$$

where

$$\Delta E(A \rightarrow A^-) = \Delta E[Z_A \rightarrow (Z_A+1)] = \sum_j \frac{E_j(Z_A+1) - E_j(Z_A)}{n_j(Z_A+1) + n_j(Z_A)} \tag{3b}$$

and a corresponding equation holds to calculate ΔE $(B \rightarrow B^+)$.

Each energy term in Eq. (3b) is the difference between the energies E_j of the valence electrons of type j (j = s,p,d,f) for the elements (Z_A+1) and Z_A, normalized to the total number of j electrons in the two elements. The s, s and d, and s and p electrons are considered when the initial compound constituents belong, respectively, to groups IA and IIA, IIIA to IIB and IIIB to VIIB of the periodic table. Positive ΔE_{e^-} (i → e) values signify that the nucleation of effective compound dimers enhances system energy with an overall destabilizing effect; by contrast, the negative parameter sign means that effective compound dimers contribute to system stability. It is remarkable that compositional changes, as assumed by the SCT model, need atomic short-range migrations over distances at most of the order of cascade radius; thus the segregation timescale is consistent with the cascade lifetime. Molecular dynamics simulations of thermal spike evolution in copper [9] show a matter wave propagating towards the cascade periphery at a typical speed of 4 nm ps^{-1}. Such a mechanism is completely different from those that dominate ion mixing, whose maximum efficiency is associated with long-range atomic migration, driven by defect migration, with timescales of many seconds after cascade formation.

A further step of the SCT model takes into account the trend in variation of a global thermochemical parameter. Given the enthalpies of formation $\Delta H_{f,i}$ of the initial compound and $\Delta H_{f,e}$ of the equiatomic effective compound, we evaluate the enthalpy change $\Delta(\Delta H_f)$ associated with effective compound nucleation

$$\Delta(\Delta H_f) = \Delta H_{f,e} - \Delta H_{f,i}. \tag{4}$$

Positive $\Delta(\Delta H_f)$ values indicate system destabilization, while negative parameter values correspond to system stabilization.

The third step of the SCT model is to calculate the local strain the target undergoes as a consequence of ion formation by a CTR. Given the prototypical unit of the A_xB_y crystal (e.g., $x < y$), with volume V_u [14] x CTRs (Eq. (2a)) yield $x(A^- + B^+)$ ions with volumes V_{A^-} [15] and V_{B^+} [16] and $(y-x)$ B neutral atoms, with volume V_B [16]. Thus the volume of CTR products V_{CTR} is

$$V_{CTR} = x(V_A^- + V_B^+) + (y-x)V_B. \tag{5}$$

The absolute value of the relative volume change $|\Delta V|_{rel}$ is calculated by comparing the volume of CTR products with the volume of the crystalline unit V_u

$$|\Delta V|_{rel} = |(V_{CTR} - V_u)/V_u|. \quad (6)$$

A high local volume change is assumed to favour material destabilization.

3. Results and discussion

Table 1 lists the initial compound, amorphized or crystalline upon ion bombardment, segregating constituent, the effective compound, ΔE_{e^-} $(i \rightarrow e), \Delta(\Delta H_f)$ [17,18] and $|\Delta V|_{rel}$. All materials were irradiated at room temperature, or slightly above, with the exception of MoO_3 which was bombarded at 77 K.

A representative set of 22 binary oxides is considered, 11 of which are reported in the literature to vitrify under some specific bombardment conditions. It is known that amorphization susceptibility is strongly affected by the nature of the bombarding ions, their energy, the dose and temperature of irradiation. In particular some compounds, both metallic and non-metallic can be vitrified at cryogenic temperatures, while they resist amorphization at room temperature. Also, we observe that a peculiar dose dependence is sometimes found; a material is completely, or partially amorphized when bombarded up to an upper threshold dose, beyond which recrystallization is observed. In case of contrasting experimental data, SCT model assumes that a compound is amorphized when at least under a specific set of experimental conditions partial or complete amorphization was observed. Of course, not for all compounds an exhaustive exploration of irradiation conditions is available, so that a compound considered crystalline on the basis of present experimental data could be amorphized in a future experiment. Referring to Table 1, among the compounds considered in this study MgO is taken as partly amorphized by 150 keV Kr ions given the observed severely disordered regions, taken as remnants of quasi-amorphous collision cascades [21], whose existence was confirmed in subsequent experiments performed with Ar ions of the same energy [26]. In the case of ZrO_2 [20] while X-ray patterns indicate that the film is a considerably disordered, distorted crystalline lattice, FTIR spectra show broad, weakly structured features which correspond to coexisting partially amorphous and distorted crystalline structures.

Vitrified oxides show positive values of both ΔE_{e^-} and $\Delta(\Delta H_f)$, while for crystalline oxides both ΔE_{e^-} and $\Delta(\Delta H_f)$ values are negative, in agreement with model predictions. In Fig. 2 ΔE_{e^-} (i → e) is plotted against $\Delta(\Delta H_f)$. Filled triangles refer to compounds vitrified by irradiation, and they all fall in the region of *positive* parameter values, while all data for crystalline compounds (filled circles) lie in the region of *negative*

Table 1
Calculated SCT model parameters for binary oxides, amorphized (a-) or crystalline (c-) upon ion bombardment

Initial (i) compound	References	Segregant [19]	Effective (e) compound	ΔE_{e^-} (i → e) (eV)	$\Delta(\Delta H_f)$ (eV at^{-1})	$\lvert\Delta V\rvert_{rel}$
a-Bi_2O_3	[2]	O	Pb F	+2.425	+0.801	0.33
a-Cr_2O_3	[2]	O	V F	+5.207	+0.373	0.64
a-Fe_2O_3	[20]	O	Mn F	+1.792	+0.204	0.41
a-GeO_2	[2]	O	Ga F	+0.756	–[a]	0.05
a-MgO	[21]	O	Na F	+1.382	+0.128	0.34
a-MoO_3	[22]	O	Nb F	+1.751	+0.057	0.42
a-Nb_2O_5	[2]	O	Zr F	+1.980	+3.683	0.40
a-SiO_2	[2]	O	Al F	+0.564	+0.516	0.32
a-TeO_2	[2]	O	Sb F	+1.202	+0.314	0.39
a-V_2O_5	[2]	O	Ti F	+1.611	+1.616	0.38
a-ZrO_2	[20]	O	Y F	+1.368	+0.315	0.48
c-Ag_2O	[2]	O	Pd F	−1.472	−4.756	0.17
c-BeO	[2]	O	Li F	−0.631	−0.542	0.68
c-CaO	[2]	O	K F	−0.194	−0.097	0.07
c-CeO_2	[23]	O	La F	−0.240	−5.485	0.28
c-Cu_2O	[2]	O	Ni F	−0.223	−2.871	0.09
c-In_2O_3	[24]	O	Cd F	−1.096	−1.715	0.16
c-PbO	[2]	O	Tl F	−1.182	−2.237	0.29
c-SnO	[2]	O	In F	−1.075	–[a]	0.24
c-TiO	[2]	O	Sc F	−0.238	−1.868	0.23
c-Y_2O_3	[25]	O	Sr F	−0.390	−2.367	0.30
c-ZnO	[2]	O	Cu F	−0.591	−3.892	0.08

[a] Heats of formation not available for Ga–F and In–F compounds.

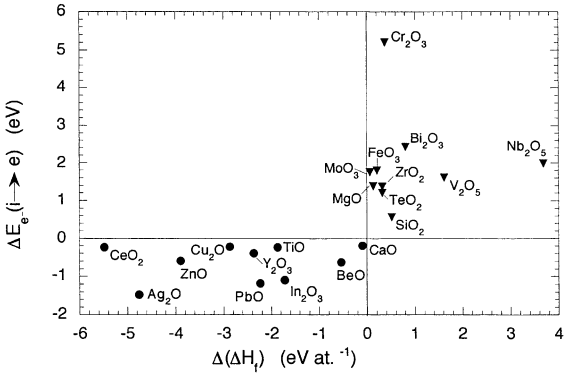

Fig. 2. Relationship between the energetic parameters $\Delta E_{e^-}(i \rightarrow e)$ and $\Delta(\Delta H_f)$ for amorphized (full triangles) and crystalline (full circles) binary oxides.

parameter values. The trend of the electronic energy contribution to effective dimer formation is in agreement with the trend of a global thermochemical parameter, $\Delta(\Delta H_f)$; this strengthens the idea that thermodynamic forces, here embodied in compound formation enthalpy, play a role in the late stages of cascade evolution.

With respect to volume changes, in Table 1a threshold $|\Delta V|_{rel}$ value of 0.3 separates amorphized oxides ($|\Delta V|_{rel} > 0.3$) from crystalline oxides ($|\Delta V|_{rel} < 0.3$). In each group one exception is found (GeO_2 and BeO, respectively). Although the threshold parameter value has no specific significance, the indication that amorphization is associated with a local dilation exceeding an upper limit is in agreement with experimentally observed strains as high as 15% in vitrified systems [27]. In Fig. 3 $\Delta(\Delta H_f)$ is represented against $|\Delta V|_{rel}$ for all oxides considered here. It is noteworthy that an old amorphizability criterion for binary metallic alloys [28] is in turn based on the idea that local lattice deformations are able to drive crystal destabilization. However, in that case

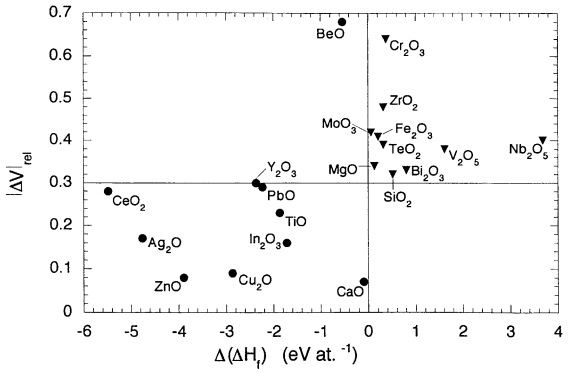

Fig. 3. Relationship between the enthalpy change $\Delta(\Delta H_f)$ and the local relative volume change $|\Delta V|_{rel}$ for amorphized (full triangles) and crystalline (full circles) binary oxides.

only the relative atomic volume difference between initial alloy constituents is considered. A relevant atomic volume mismatch is supposed to result in steric hindrances which impede the attainment of specific crystal structures during quenching from the melt. By contrast, in the SCT model the volume occupied by a prototypical unit of unirradiated crystalline compound is compared to the volume of compound constituents after dissociation and ionization processes have occurred at the cascade–matrix interface.

In conclusion, energy, enthalpy and volume changes induced by a CTR all show threshold values which allow separation of crystalline from vitrified oxides. As the basic mechanisms that determine cascade evolution over the timescale considered in SCT model are the same in non-metallic compounds as in metals, SCT model provides a unified framework to study the structural evolution under ion bombardment in either class of materials.

Acknowledgements

This research was supported by CNR-Progetto Finalizzato Materiali Speciali per Tecnologie Avanzate II.

References

[1] A. Hamberg, Geol. Förh. 36 (1914) 31.
[2] H.M. Naguib, R. Kelly, Radiat. Eff. 25 (1975) 1.
[3] H. Inui, H. Mori, H. Fujita, Acta Metall. 37 (1989) 1337.
[4] M.G. Beghi, C.E. Bottani, P.M. Ossi, R. Pastorelli, M. Poli, B.K. Tanner, B.X. Liu, Surf. Coat. Technol. 100–101 (1998) 324.
[5] A. Benyagoub, L. Thomé, Phys. Rev. B38 (1988) 10205.
[6] P.M. Ossi, Philos. Mag. B79 (1999) 2129.
[7] P.M. Ossi, R. Pastorelli, Surf. Coat. Technol. 125 (2000) 61.
[8] P.M. Ossi, Surf. Coat. Technol. 83 (1996) 43.
[9] H. Van Swygenhoven, A. Caro, Phys. Rev. Lett. 70 (1993) 2098.
[10] P.M. Ossi, Surf. Sci. 201 (1988) L519.
[11] B.J. Garrison, H. Winograd, D. Lo, T.A. Tombrello, M.H. Shapiro, D.E. Harrison Jr., Surf. Sci. 180 (1987) L129.
[12] U. Mizutani, M. Sasaura, U. Yamada, T. Matsuda, J. Phys. F 17 (1987) 667.
[13] A.A. Radzig, B.M. Smirnov, Reference Data on Atoms, Molecules and Ions, Springer, Berlin, 1985.
[14] Metals and Alloys Indexes, International Centre for Diffraction Data, Swarthmore, PA, 1992.
[15] K.D. Sen, P. Politzer, J. Chem. Phys. 91 (1989) 5123.
[16] Periodic Table of the Elements, IUPAC, 1998.
[17] F.R. de Boer, R. Boom, W.C.M. Mattens, A.R. Miedema, A.K. Niessen, Cohesion in Metals: Transition Metal Alloys, North-Holland, Amsterdam, 1989.
[18] I. Barin, Thermochemical Data of Pure Substances, VCH, Weinheim, 1989.

[19] A. Zangwill, Physics at Surfaces, Cambridge University Press, Cambridge, 1988, p. 11.
[20] A.R. González-Elipe, F. Yubero, J.P. Esponós, A. Caballero, M. Ocańa, J.P. Holgado, J. Morales, Surf. Coat. Technol. 125 (2000) 116.
[21] E. Friedland, Nucl. Instrum. and Meth. B 85 (1994) 316.
[22] S. Furuno, H. Otsu, K. Hojou, K. Izui, Nucl. Instrum. and Meth. B 107 (1996) 223.
[23] M. Satoh, Y. Yamamoto, T. Inoue, Nucl. Instrum. and Meth. B 127/128 (1997) 166.
[24] I. Nakamura, M. Kamiya, I. Takano, Y. Sawada, E. Nakazawa, Surf. Coat. Technol. 103–104 (1998) 83.
[25] A. Traverse, P. Parent, J. Mimault, N. Thromat, M. Gautier, J.P. Durand, A.M. Flank, A. Quivy, A. Fontaine, Nucl. Instrum. and Meth. B 86 (1994) 270.
[26] E. Friedland, Nucl. Instrum. and Meth. B 116 (1996) 136.
[27] L.W. Hobbs, J. Non-Cryst. Solids 182 (1995) 27.
[28] T. Egami, Y. Waseda, J. Non-Cryst. Solids 64 (1984) 113.